Modeling a Hand Prosthesis with Word Bond Graph Objects

Anand Vaz
Department of Mechanical Engineering
SLIET, Longowal, District Sangrur
Punjab 148106, India
Email: anandvaz@ieee.org

Shinichi Hirai
Department of Robotics
Ritsumeikan University, Noji-higashi 1-1-1
Kusatsu, Shiga 525-8577, Japan
Email: hirai@se.ritsumei.ac.jp

Abstract - The bond graph approach is used to model a hand prosthesis system, which is quite large to represent conveniently using either single or multibond graphs. This is usually the case with modeling biomechanical systems. To facilitate compact modeling of this system, the concept of Word Bond Graphs is applied to represent component subsystems as Objects. Such Word Bond Graph Objects (WBGO) are compact representations of subsystems, within the overall system, and have a well defined structure. They preserve an understanding of the physical system while facilitating quick and easy programming for numerical simulations due to their object oriented structure. WBGO identified and analyzed here for the hand prosthesis system include rigid finger link dynamics, translational and rotational coupling between two consecutive finger links, and string-tube mechanics for *passive prosthetic joint* actuation by natural *active joints*. The bond graph details for each WBGO have been presented together with a derivation of their system equations. The WBGO are then used to integrate a complete assembly of the dynamics of the hand prosthesis system.

I. Introduction

Biomechanical systems, and especially prosthetic systems, are usually large with interconnections and are applications well suited to bond graph modeling. The method of Bond graphs is an attractive and powerful technique as it offers a unified framework for modeling the mechanism, and, the actuation and control systems due to its capability of handling multi-energy domains [Karnopp et al., 2000], [Mukherjee and Karmakar, 2000]. In this work the bond graph technique is applied to the important area of modeling the essential mechanism of a human hand with a view to the design and development of hand prosthesis. The prostheses considered in this work have been proposed earlier by the authors [Vaz and Hirai, 2003], and are based on actuation of prosthetic fingers by the remaining natural fingers of a partially impaired hand.

However, the dynamics for a hand-prosthesis system, using 1-bonds or scalar bonds, would yield a bond graph too large to represent and analyze. Vector bond graphs (VBG) or multibond graphs (MBG) do help to compact the representation to some extent [Bonderson, 1975], [Bonderson, 1977], [Breedveld, 1982], [Breedveld 1985]. It would be preferable to have more compact representation which preserves a clear picture of the overall system and can be explored analytically.

One way to achieve this is to consider the overall system model as an integrated assembly of component subsystems which can interact with each other. Subsystems whose structure appears more than once in a system can be identified as a Word Bond Graph Object (WBGO). Word Bond Graphs (WBG) have been used extensively in literature to represent models of subsystem dynamics [Karnopp et al., 2000], [Breedveld 1985], [Tiernego and Bos, 1985], [Bos and Tiernego, 1985].

WBG have an inherent structure which can be put to effective use. The detailed structure of a WBG can be modeled using a combination of MBG and scalar bond graphs. The structure may or may not be assigned a fixed causality. The WBG can be treated as an Object with well defined input and output variables, state variables and parameters. Inputs and outputs to WBG structure using conventional bond graph variables of efforts and flows can be made explicit and used as handles for interfacing with other Objects or bond graph elements. The resulting structure of the WBG has properties of Objects as used in Object oriented programming. Code for simulation based on WBGO can be developed systematically and rapidly, or existing bond graph software can be used to exploit this structure. Hence it will be appropriate to distinguish them as WBGO. Interaction between these WBGO is graphically represented using scalar bonds or multibonds as in usual bond graph methodology. Once a WBGO with its interface is defined, it can be used as a component in the assembly of a complete system. Thus WBGO facilitate modeling of large and complex systems, in a graphical and intuitive manner.

Applying this concept to the modeling of a hand prosthesis system requires an identification of the possible subsystems which can be represented using WBGO. Modeling of the hand prosthesis can be initiated from its fingers. These may be considered to be made up of almost rigid links (bones called phalanges). The joints between links are generally revolute, though not in a strict kinematic sense. The joints are roughly spherical in the

kinematic sense but have a prominent revolute motion about an axis. The rigid constraints at joints are relaxed due to the presence of soft tissue and fluid [Chao et al., 1989]. We can therefore consider a finger joint as connecting two links and permitting their revolute motion about its axis. The model of the dynamics of the hand and prosthesis system can be obtained by assembling WBGO for the following subsystems: (1) dynamics of each rigid finger link, (2) the translational and rotational couplings between two consecutive finger links, and, (3) the string-tube mechanism which transmits motion from an active natural joint to a passive prosthetic joint.

The detailed structure of each of these WBGO is worked out in subsequent sections so that their integration into a complete assembled model is made possible. Although the presentation pertains to the modeling of hand prosthesis designs proposed by the authors, the techniques are quite general and can be applied to other prosthetic devices and robotic systems as well.

Organization of this paper is as follows. The next section clarifies the notation adopted in this work. In section II, a preview of rigid body mechanics using multibond graphs, is presented. WBGO for the hand prosthetic systems are systematically developed from the framework of multibond graphs in section III. The structure of a WBGO from the perspective of bond graphs as well as object-oriented programming is also explained in this section. Here, the complete integration of component subsystems with each other is achieved to obtain a compact system dynamics model for the hand prosthesis system. Section IV offers concluding remarks.

NOMENCLATURE

The notation followed here for representation of mathematical quantities is based on an adaptation from [Craig, 1989] which is well known especially in robotics literature. Vectors are shown with a bar above. ${}^{0}_{Q}\overline{r}_{P}$ represents the position vector of a point ***P*** observed with respect to point ***Q*** and expressed in the frame ***0***. Other notation is as tabulated below.

F_i =Tension force in string *i*; *i* = 1, 2; $\in \mathbb{R}^1$

${}^{0}\overline{F}_{P}$ =Force vector acting at point ***P***, expressed in inertial frame ***0***; $\in \mathbb{R}^3$

$\left[{}^{0}_{C_i}I_i \right]$ =Inertia tensor of link *i* with respect to its center of mass, expressed in inertial frame ***0***; $\in \mathbb{R}^{3\times3}$

$\left[{}^{0}_{C_i}I_i \right]^{-1}$ =Inverse of inertia tensor $\left[{}^{0}_{C_i}I_i \right]$; $\in \mathbb{R}^{3\times3}$

K_{s_i} =Stiffness of string-tube *i*; *i* = 1, 2; $\in \mathbb{R}^1$

R_{s_i} =Damping coefficient of string-tube *i*; *i* = 1, 2; $\in \mathbb{R}^1$

$\left[K_{i-1,i} \right]$ =Translational stiffness matrix at joint coupling between link *i* and *i-1*; $\in \mathbb{R}^{3\times3}$

M_i =Mass of link *i*.

$\left[M_i \right] = M_i \left[U \right]$; $\in \mathbb{R}^{3\times3}$. $\left[U \right] \in \mathbb{R}^{3\times3}$ is a unit matrix

$\left[M_i \right]^{-1}$ =Matrix inverse of $\left[M_i \right]$; $\in \mathbb{R}^{3\times3}$

$\left[R_{i-1,i} \right]$ =Translational damping matrix at joint coupling between link *i* and *i-1*; $\in \mathbb{R}^{3\times3}$

${}^{0}_{C}R$ =Rotation matrix describing orientation of frame ***C*** with respect to inertial frame ***0***; $\in \mathbb{R}^{3\times3}$

${}^{0}_{C}\dot{R}$ =Time derivative of ${}^{0}_{C}R$; $\in \mathbb{R}^{3\times3}$

${}^{0}_{A}R^{T}$ =Transpose of rotation matrix ${}^{0}_{A}R$

${}^{0}\overline{p}_i$ =Translational momentum of link *i* observed and expressed in the inertial frame ***0***.

${}^{0}_{C_i}\overline{p}_i$ =Angular momentum vector of link *i* with respect to its center of mass and expressed in inertial frame ***0***.

r_{iA} =Radius of pulley at active joint on which string *i* winds; *i* = 1, 2.

r_{iP} =Radius of pulley at passive joint on which string *i* winds; *i* = 1, 2.

${}^{0}_{C_i}\overline{r}_{P_i}$ =Position vector of point ***P*** on link *i* with respect to its center of mass and expressed in the inertial frame ***0***.

$\left[{}^{0}_{C_i}\overline{r}_{P_i} \times \right]$ =Skew symmetric cross product matrix obtained from vector ${}^{0}_{C_i}\overline{r}_{P_i}$; $\in \mathbb{R}^{3\times3}$

${}^{0}_{P_i}\overline{r}_{P_{i-1}}$ =Position of point $\boldsymbol{P_{i-1}}$, at the joint, on link *i-1* with respect to its corresponding position $\boldsymbol{P_i}$ on link *i*, expressed in inertial frame ***0***.

${}^{0}_{P_i}\dot{\overline{r}}_{P_{i-1}}$ =Relative velocity of point $\boldsymbol{P_{i-1}}$, at the joint, on link *i-1* with respect to point $\boldsymbol{P_i}$ on link *i*, expressed in inertial frame ***0***.

${}^{0}_{0}\dot{\overline{r}}_{C_i}$ =Velocity of center of mass of the i^{th} link observed and expressed in inertial frame ***0***.

${}^{A}_{B}\dot{\overline{r}}_{C} = \frac{d}{dt}\left\{ {}^{A}_{B}\overline{r}_{C} \right\}$; time derivative of ${}^{A}_{B}\overline{r}_{C}$; $\in \mathbb{R}^3$

${}^{0}\hat{u}_{C_i}$ =i^{th} column of ${}^{0}_{C}R$ representing unit vector of frame ***C*** with respect to frame ***0***. $i = 1,\ 2,\ 3$.

τ_A =Torque input to the string-tube mechanism by the active joint; $\in \mathbb{R}^1$

τ_P =Torque applied by the string-tube mechanism on the passive joint; $\in \mathbb{R}^1$

τ_{Az_i} =Torque input to the string-tube mechanism by the active joint *i* about its axis; $\in \mathbb{R}^1$

${}^{i-1}\tau_{z_i}$ =Z component of torque input to the active joint *i* about its axis, expressed in frame *i-1*; $\in \mathbb{R}^1$

${}^{i-1}\tau_{z_i\text{in}}$ =Component of torque input by the natural finger to the active joint *i* about its axis, expressed in frame *i-1*; $\in \mathbb{R}^1$

${}^{i-1}\overline{\tau}_i$ =Torque applied on link *i* expressed in frame *i-1*; $\in \mathbb{R}^3$

${}^{0}\overline{\tau}_i$ =Torque applied on link *i* with respect to and expressed in inertial frame ***0***; $\in \mathbb{R}^3$

$\dot{\theta}_A$ =Active joint angle rate ; $\in \mathbb{R}^1$

$\dot{\theta}_p$ =Passive joint angle rate; $\in \mathbb{R}^1$

${}^A_B\overline{\omega}_C$ =Angular velocity vector of frame ***C*** with respect to frame ***B*** and expressed in frame ***A***; $\in \mathbb{R}^3$

$\left[{}^A_B\overline{\omega}_C \times\right]$ =Skew symmetric cross product matrix obtained from angular velocity vector ${}^A_B\overline{\omega}_C$; $\in \mathbb{R}^{3\times 3}$

Δs_i =Extension of string *i*; *i* = 1, 2.

$\Delta \dot{s}_i$ =Time rate of extension of string *i*; *i* = 1, 2.

In this work, a scalar and multibond (vector bond) are differentiated by their relative thickness as shown in Fig. 1. A multibond is an ordered collection of three scalar bonds. Hence the dimension three is not explicitly indicated on the vector bond. This is also to avoid congestion in figures. Thus, if the flow vector $\overline{f} = \dot{\overline{r}}_C$ then $\{f_1, f_2, f_3\}^T = \{v_{Cx}, v_{Cy}, v_{Cz}\}^T$, where $\overline{f} = \{f_1, f_2, f_3\}^T$ and $\dot{\overline{r}}_C = \{v_{Cx}, v_{Cy}, v_{Cz}\}^T$. Similarly, if the effort vector $\overline{e} = \overline{F}_C$ then $\{e_1, e_2, e_3\}^T = \{F_{Cx}, F_{Cy}, F_{Cz}\}^T$, where $\overline{e} = \{e_1, e_2, e_3\}^T$ and $\overline{F}_C = \{F_{Cx}, F_{Cy}, F_{Cz}\}^T$.

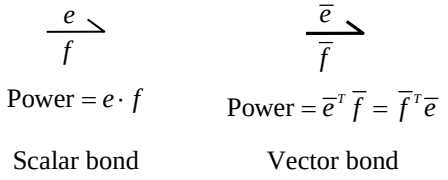

Fig. 1. Convention used for scalar and vector bonds

The notation used here is thus slightly different from that used by [Breedveld, 1985], [Tiernego and Bos, 1985], [Bos and Tiernego, 1985]. Moreover, the solid bond is easier to draw than the usual multibond with two parallel lines and its bond strength indicated in between them.

The notation for the modulated transformer is shown in Fig. 2. The modulus is detached from the power directions of multibonds. A curved arrow is used to clarify the relationships between flow and effort vectors.

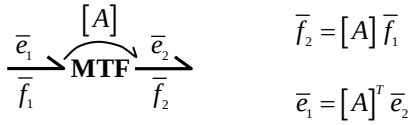

Fig. 2. Notation for the modulated transformer.

II. BOND GRAPH PREVIEW FOR RIGID BODY MECHANICS

One of the basic subsystems in the hand prosthesis system is the finger link, which is considered as a rigid body. In this section, a review of rigid body dynamics is presented. This will be used in the development of WBGO subsequently.

A. Translation and rotation

The fundamental equations of motion for rigid bodies [Shames, 1996] can be represented using bond graphs as shown. Translation of an unconstrained rigid body ***B*** is depicted using the multibond graph representation of Fig. 3.

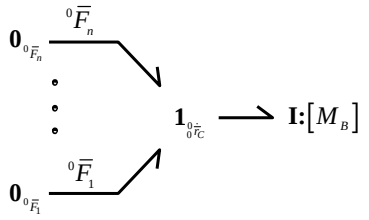

Fig. 3. Multibond graph for the Newton's second law applied to the rigid body

$\mathbf{1}_{{}_0^0\dot{\overline{r}}_C}$ is the common flow junction with the velocity of the center of mass (CM) ***C***, ${}_0^0\dot{\overline{r}}_C$, as the common flow vector in all bonds connected to it. Fig. 3 shows that the translational momentum of the entire rigid body ***B*** can be considered to be concentrated at the center of its mass, and it changes according to the resultant of the forces applied on it.

$$\frac{d}{dt}{}^0\overline{p}_B = \sum_i {}^0\overline{F}_i \qquad (1)$$

where, ${}^0\overline{p}_B = \left\{M_B\, {}_0^0\dot{\overline{r}}_C\right\}$ is the translational momentum vector of the rigid body, and M_B is its mass. The momentum is expressed in the inertial frame ***0***. $[M_B] = M_B[U]$, where $[U]$ is a 3×3 unit matrix.

Rotational motion of the body, with frame ***B*** fixed on it, is given by the bond graph of Fig. 4. It clearly represents the cause-effect relationship between torque acting on the unconstrained rigid body and the angular momentum about its center of mass (CM) ***C***. The total torque acting on the rigid body about ***C*** causes a change in its angular momentum about ***C***. The effect is the rotation of the body with angular velocity ${}_0^0\overline{\omega}_B$, and is decided by the inertial properties of the rigid body.

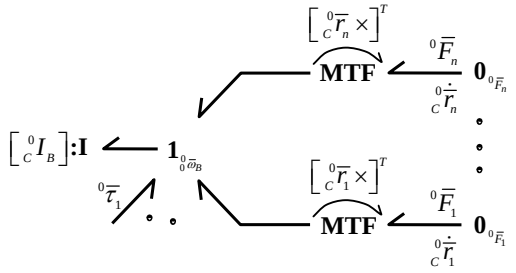

Fig. 4. Multibond graph for rotational motion of the rigid body.

The equation for rotation of the rigid body, due to forces and torques acting on it, as represented in the bond graph can be written as

$$\frac{d}{dt}\,{}^{0}_{C}\overline{p}_{B} = \sum_{i}\left[{}^{0}_{C}\overline{r}_{i}\times\right]{}^{0}\overline{F}_{i} + \sum_{j}{}^{0}\overline{\tau}_{j} \tag{2}$$

where, ${}^{0}_{C}\overline{p}_{B} = \left\{\left[{}^{0}_{C}I_{B}\right]{}^{0}_{0}\overline{\omega}_{B}\right\}$ is the angular momentum of the body ***B*** about its CM ***C***, and is expressed in the inertial frame ***0***. $\left[{}^{0}_{C}I_{B}\right]$ is the inertia tensor of the body ***B*** expressed in the frame ***0***. $\left[{}^{0}_{C}\overline{r}_{i}\times\right]$ is the skew symmetric matrix obtained from vector ${}^{0}_{C}\overline{r}_{i} = \left\{{}^{0}_{C}x_{i} \quad {}^{0}_{C}y_{i} \quad {}^{0}_{C}z_{i}\right\}^{T}$ as,

$$\left[{}^{0}_{C}\overline{r}_{i}\times\right] = \begin{bmatrix} 0 & -{}^{0}_{C}z_{i} & {}^{0}_{C}y_{i} \\ {}^{0}_{C}z_{i} & 0 & -{}^{0}_{C}x_{i} \\ -{}^{0}_{C}y_{i} & {}^{0}_{C}x_{i} & 0 \end{bmatrix} \tag{3}$$

From above, both translation and rotation for the rigid body can be combined in one bond graph as shown in Fig. 5. It may be noted that the initial structure of this model is based on the kinematic relations given by

$${}^{0}_{0}\dot{\overline{r}}_{i} = {}^{0}_{0}\dot{\overline{r}}_{C} + \left[{}^{0}_{C}\overline{r}_{i}\times\right]^{T}{}^{0}_{0}\overline{\omega}_{B}, \qquad i = 1,..,n. \tag{4}$$

It may be noted that the Bond graph for the unconstrained rigid body can be integrally causalled.

Since the elements of the inertia tensor $\left[{}^{0}_{C}I_{B}\right]$ are expressed in the frame ***0*** they change due to rotation of

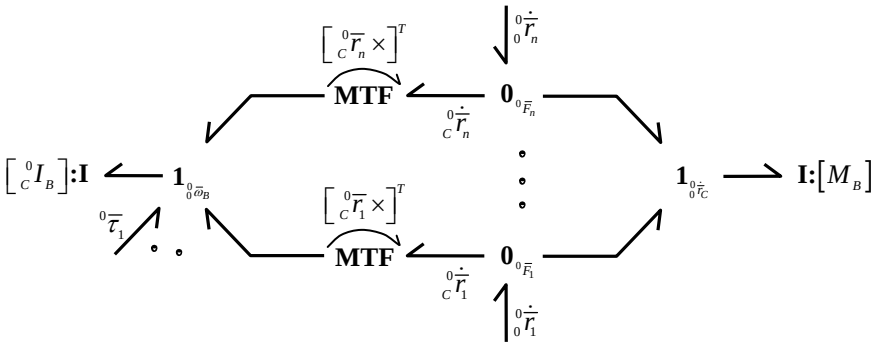

Fig. 5. Multibond graph representing translation and rotation of an unconstrained rigid body.

the body with respect to frame ***0***. We know that the elements of the inertia tensor are constant for the rigid body if expressed in a frame fixed on the body itself. The inertia tensor expressed in frame ***0*** can be related to that in frame ***B*** as

$$\left[{}^{0}_{C}I_{B}\right] = {}^{0}_{B}R\left[{}^{B}_{C}I_{B}\right]{}^{0}_{B}R^{T} \tag{5}$$

An alternative representation to (2) can be expressed in the body frame ***B*** as,

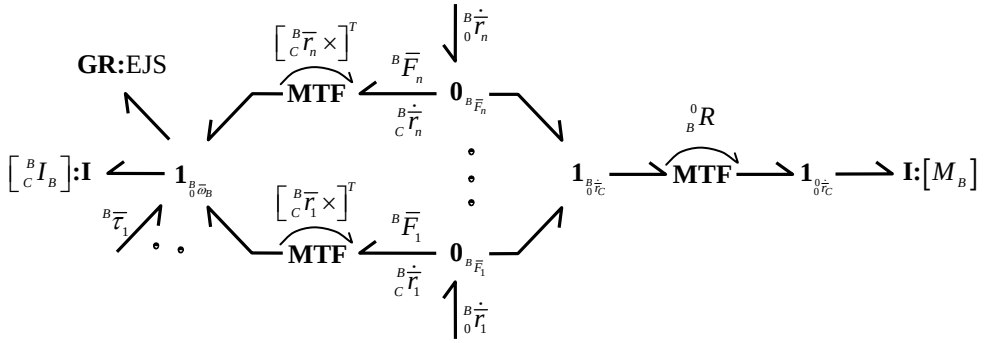

Fig. 6. Multibond graph model of an unconstrained rigid body. The rotational motion is expressed in the body frame ***B***, while translational motion is expressed in the inertial frame ***0***.

$$\frac{d}{dt}\,{}^{B}_{C}\overline{p}_{B} = \left[{}^{B}_{C}\overline{p}_{B}\times\right]{}^{B}_{0}\overline{\omega}_{B} + \sum_{i}\left[{}^{B}_{C}\overline{r}_{i}\times\right]{}^{B}\overline{F}_{i} + \sum_{j}{}^{B}\overline{\tau}_{j} \qquad (6)$$

The corresponding multibond graph is shown in Fig. 6. In (6), ${}^{B}_{C}\overline{p}_{B} = \left\{\left[{}^{B}_{C}I_{B}\right]{}^{B}_{0}\overline{\omega}_{B}\right\}$ is the angular momentum of the body ***B*** about its CM ***C***, and is expressed in the body frame ***B***. $\left[{}^{B}_{C}\overline{p}_{B}\times\right]$ is the skew symmetric matrix obtained from vector ${}^{B}_{C}\overline{p}_{B}$, as shown in (3). The elements of the inertia tensor $\left[{}^{B}_{C}I_{B}\right]$ are constants. When the body frame ***B*** is chosen to coincide with the principal axes of inertia, $\left[{}^{B}_{C}I_{B}\right]$ becomes diagonal. The first term on the right hand side of (6) has the operator $\left[{}^{B}_{C}\overline{p}_{B}\times\right]$ which when operated on the flow vector ${}^{B}_{0}\overline{\omega}_{B}$ provides the gyroscopic term corresponding to the Euler junction structure (EJS) [Karnopp et al., 2000] represented by the gyristor multiport element **GR** [Tiernego and Bos, 1985], [Bos and Tiernego, 1985]. On account of the cross product terms occurring in the modulated transformers due to kinematics, in bond graph models of Fig. 5 and Fig. 6, these cannot be considered as entirely acausal [Favre and Scavarda, 1998].

The designer has the option to choose any one of the two frames, frame ***0*** or frame ***B***, for expression of rotational motion. From the computational viewpoint, both the options require the same number of scalar multiplications, with the former option requiring marginally lesser number of additions. Hence we choose to use representation in the inertial frame ***0***. Other options may exist depending on the configuration of the mechanism modeled. Considerations for the choice of representation frames from the viewpoint of kinematic loops have been discussed by [Favre and Scavarda, 1998].

The orientation matrix ${}^{0}_{B}R$ is necessary in either of the two viewpoints mentioned above, and is discussed in the next subsection.

B. Orientation

The orientation of frame ***B*** with respect to frame ***0***, given by the rotation matrix ${}^{0}_{B}R$, is obtained by the integration of the matrix differential equation

$${}^{0}_{B}\dot{R} = \left[{}^{0}_{0}\overline{\omega}_{B}\times\right]{}^{0}_{B}R \qquad (7)$$

This means that if the orientation of the rigid body at time t_0 is given as ${}^{0}_{B}R(t_0)$, the orientation at time t can be obtained as ${}^{0}_{B}R(t)$ from integration of (7). Information about ${}^{0}_{0}\overline{\omega}_{B}$ is necessary. There are well known

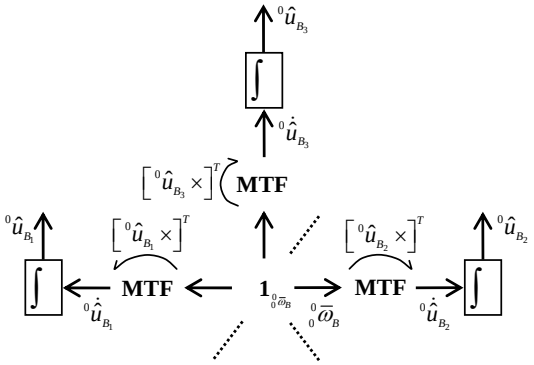

Fig. 7. Obtaining columns of the orientation matrix ${}^{0}_{B}R$.

dependencies among the elements of ${}^{0}_{B}R$ due to its orthonormality. The columns of ${}^{0}_{B}R$ are unit vectors of frame ***B*** along its coordinate axes expressed in the frame ***0***. Due to the angular velocity ${}^{0}_{0}\overline{\omega}_{B}$ of the body, these unit vectors undergo a change of orientation, at time t, with respect to frame ***0***. The columns are obtained from integration of

$${}^{0}\dot{\hat{u}}_{B_i} = \left[{}^{0}\hat{u}_{B_i}\times\right]^{T}{}^{0}_{0}\overline{\omega}_{B}, \quad i = 1,\ 2,\ 3 \qquad (8)$$

where, ${}^{0}_{B}R = \left[{}^{0}\hat{u}_{B_1}\quad {}^{0}\hat{u}_{B_2}\quad {}^{0}\hat{u}_{B_3}\right]$. In terms of Bond graphs, this relationship is shown in Fig. 7. Thus the orientation matrix ${}^{0}_{B}R$ can be constructed again. This approach has redundancy in it, caused by the orthonormal nature of ${}^{0}_{B}R$. The third column vector of ${}^{0}_{B}R$ can be obtained from

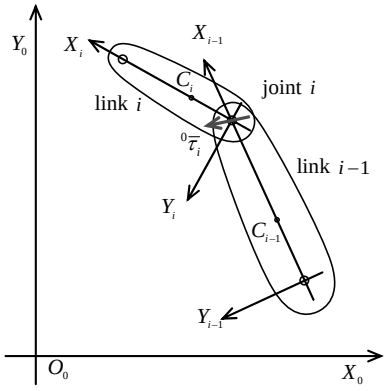

Fig. 8. A finger joint connecting two links.

the previous two columns by vector cross multiplication.

The relative orientation between two links, say ***A*** and ***B***, can be obtained from (9) once their orientations ${}^{0}_{A}R$ and ${}^{0}_{B}R$, with respect to frame ***0***, are known.

$${}^{A}_{B}R = {}^{0}_{A}R^{T}\,{}^{0}_{B}R \qquad (9)$$

III. Construction of Word Bond Graph Objects for the Hand Prosthesis System

The above developments are applied to an example of a finger with a revolute joint, shown in Fig. 8.

A. WBGO for the two-link finger

The MBG for the system is shown in Fig. 9. The WBGO for two consecutive links *i* and *i-1* are outlined in the MBG of Fig. 9. *P* is the point of connection between the two links if the translational constraint is rigid. The constraint is relaxed by using an elastic coupling. In this case the point on link *i* coinciding with point *P* is P_i, and on link *i-1* is P_{i-1}. The significance of elastic elements in relaxing rigid constraints has been explained using scalar bond graphs in [Karnopp, 1997] and [Zeid and Overholt, 1995]. The MBG has integral causality, due to relaxation of kinematic constraints. If the constraints were to be rigidly imposed, derivative causality would appear at the multibonds connected to the translational inertia elements. Derivative causality occurs due to the imposition of kinematic constraints which result in the dependence of the momenta of masses M_1 and M_2 on the angular momenta of links 1 and 2 about their respective centers of mass. In natural finger systems, the presence of soft tissue and fluid relax the joint constraints by introducing their own properties of stiffness and dissipation. This justifies the introduction of bond graph elements representing stiffness and dissipation at respective joints.

Equations governing behavior of the finger joint system are derived systematically from the bond graph of Fig. 9 as follows.

Step I:

$$ {}^0_0\overline{\omega}_i = \left[{}^0_{C_i}I_i \right]^{-1} {}^0_{C_i}\overline{p}_i, \tag{10} $$

where, $\left[{}^0_{C_i}I_i \right]^{-1} = {}^0_iR \left[{}^i_{C_i}I_i \right]^{-1} {}^0_iR^T$.

$$ {}^0_0\overline{\omega}_{i-1} = \left[{}^0_{C_{i-1}}I_{i-1} \right]^{-1} {}^0_{C_{i-1}}\overline{p}_{i-1}, \tag{11} $$

where, $\left[{}^0_{C_{i-1}}I_{i-1} \right]^{-1} = {}^0_{i-1}R \left[{}^{i-1}_{C_{i-1}}I_{i-1} \right]^{-1} {}^0_{i-1}R^T$.

$$ {}^0_0\dot{\overline{r}}_{C_i} = \left[M_i \right]^{-1} {}^0\overline{p}_i \tag{12} $$

$$ {}^0_0\dot{\overline{r}}_{C_{i-1}} = \left[M_{i-1} \right]^{-1} {}^0\overline{p}_{i-1} \tag{13} $$

$$ {}^0\overline{F}_P = \left[K_{i-1,i} \right] {}^0_{P_i}\overline{r}_{P_{i-1}} + \left[R_{i-1,i} \right] {}^0_{P_i}\dot{\overline{r}}_{P_{i-1}} \tag{14} $$

Step II:

$$ {}^0_{C_i}\dot{\overline{p}}_i = {}^0\overline{\tau}_i + \left[{}^0_{C_i}\overline{r}_{P_i} \times \right] {}^0\overline{F}_P \tag{15} $$

$$ {}^0_{C_{i-1}}\dot{\overline{p}}_{i-1} = -{}^0\overline{\tau}_i + \left[{}^0_{C_{i-1}}\overline{r}_{P_{i-1}} \times \right] \left\{ -{}^0\overline{F}_P \right\} \tag{16} $$

$$ {}^0\dot{\overline{p}}_i = {}^0\overline{F}_P \tag{17} $$

$$ {}^0\dot{\overline{p}}_{i-1} = -{}^0\overline{F}_P \tag{18} $$

$$ \begin{aligned} {}^0_{P_i}\dot{\overline{r}}_{P_{i-1}} &= {}^0_0\dot{\overline{r}}_{P_{i-1}} - {}^0_0\dot{\overline{r}}_{P_i} \\ &= {}^0_0\dot{\overline{r}}_{C_{i-1}} - \left[{}^0_{C_{i-1}}\overline{r}_{P_{i-1}} \times \right] {}^0_0\overline{\omega}_{i-1} - {}^0_0\dot{\overline{r}}_{C_i} + \left[{}^0_{C_i}\overline{r}_{P_i} \times \right] {}^0_0\overline{\omega}_i \end{aligned} \tag{19} $$

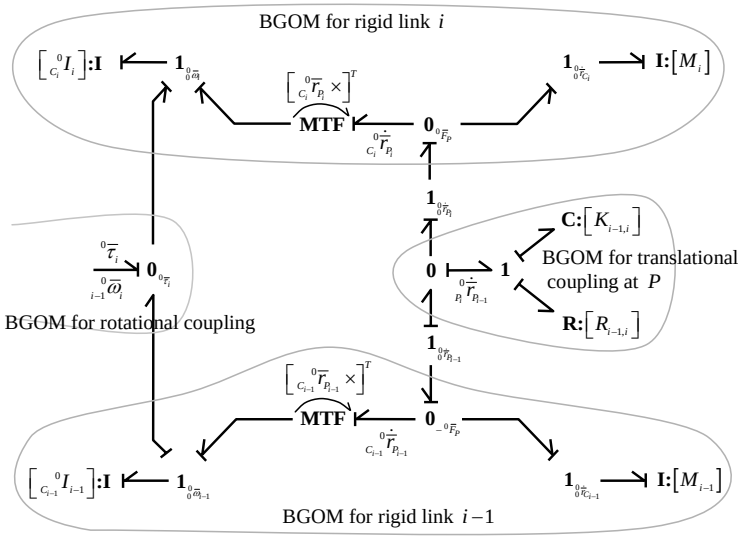

Fig. 9. Multibond graph for the finger joint system. WBGO are identified and marked.

$$ {}^0_i\dot{R} = \left[{}^0_0\overline{\omega}_i \times \right] {}^0_iR \quad \text{and,} \quad {}^0_{i-1}\dot{R} = \left[{}^0_0\overline{\omega}_{i-1} \times \right] {}^0_{i-1}R \qquad (20) $$

Each WBGO for the rigid link, identified by an outline in Fig. 9, has a well defined structure as shown in Table I.

TABLE I

Output = WBGO for link *i* (Input)

Parameters of the WBGO:	
	$\mathbf{I}:\left[M_i\right]$, $\mathbf{I}:\left[{}^0_{C_i}I_i \right]$
Initially required variables: (These are then obtained at every integration step from the solver)	
	${}^0_0\overline{r}_{C_i}$, ${}^0_iR$
Input: (can be in any or both of the following two forms)	
${}^0\overline{\tau}_i$ or	Input torque on link *i*. More than one torque can act on link *i* at a time.
$({}^0\overline{F}_P, {}^i_{C_i}\overline{r}_{P_i})$, …	Ordered pair of the force acting on link *i* at point *P*, with its corresponding position with respect to the CM of link *i*, expressed in frame *i*.
Output: (These are provided as input to the solver at every integration step)	
	${}^0_0\overline{\omega}_i$, ${}^0_0\dot{\overline{r}}_{C_i}$, ${}^0_0\dot{\overline{r}}_{P_i}$, …

The structure of the WBGO for a translational coupling is shown in Table II.

TABLE II

Output = WBGO for translational coupling between links *i* and *i-1* (Input)

Parameters:	$\mathbf{C}:\left[K_{i-1,i}\right]$, $\mathbf{R}:\left[R_{i-1,i}\right]$
Initially required variables:	${}^0_0\overline{r}_{P_i}$, ${}^0_0\overline{r}_{P_{i-1}}$
Input:	${}^0_0\dot{\overline{r}}_{P_i}$, ${}^0_0\dot{\overline{r}}_{P_{i-1}}$
Output:	${}^0\overline{F}_P$

B. WBGO for string-tube based joint actuation

The transmission of motion from the *active* to the *passive joint* of the prosthesis is discussed next. The details of actuation from the *active* to the *passive joint* have been explained in [Vaz and Hirai, 2003]. A brief review is provided here. Fig. 10 shows the string-tube based mechanism for actuation of a *passive* prosthetic joint by an *active* natural joint. Each pair of joints is connected by two string-tubes. Multi-strand wire is used for the string which passes through a steel spring-tube. The tubes are flexible but offer very high impedance to compression in the axial direction. At a joint, the tube ends are fixed on the proximal link, while the string ends are fixed on the corresponding distal link. The strings move relative to their corresponding tubes when actuated. The strings can be set with a desired initial pretension. The sense of winding of strings around pulleys at each joint determines the configuration of the mechanism. Fig. 10 shows the prosthesis joint actuation for the *unlike configuration*. Here the sense of rotation of the *passive joint* opposes that of the *active joint*, and is commonly employed for tasks such as gripping, pinching, holding, etc.

The mechanics of the string-tube connection between an *active* and a *passive joint* is shown in the bond graph of Fig. 10 [Vaz and Hirai, 2004]. The WBGO for string-tube mechanics is outlined in the figure. The two string-tubes are represented by the two paths between junctions $\mathbf{1}_{\dot{\theta}_A}$ and $\mathbf{1}_{\dot{\theta}_P}$. The **TF** elements relate string tensions to corresponding torques applied at the joints. They also relate the speeds of string motion at pulleys to corresponding joint angle rates. The modulus of each **TF** element is based on the radius of the joint pulley on which the corresponding string is wound, and on the sense of the winding. The string-tube connecting an *active* and *passive joint* decides the string tensions and hence the torques experienced on the joints based on the extension of the string-tubes. This extension is decided by the angular motions of the joints connected by the string-tubes. Multiport elements $\mathbf{C}:K_s$ and $\mathbf{R}:R_s$ are used to model elastic and dissipative behavior respectively, for each of the string-tubes. Flows $\dot{\theta}_A$ and $\dot{\theta}_P$ are input to the WBGO and efforts τ_A and τ_P are output from it.

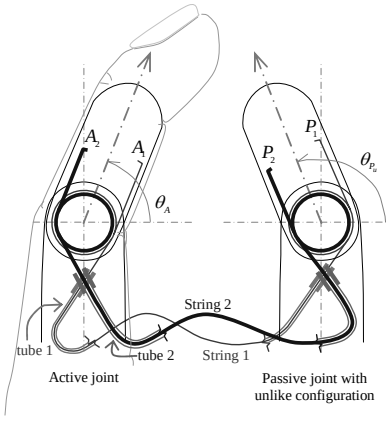

Fig. 10. Joint actuation using string-tube based system in *unlike configuration.*

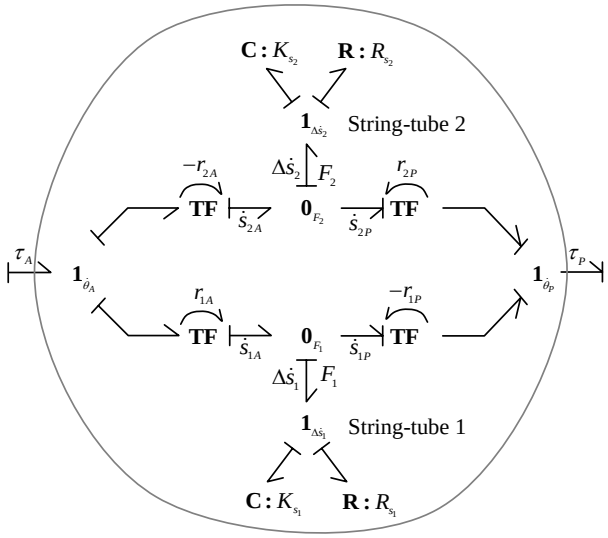

Fig. 11. String-tube mechanics. This bond graph is constructed using scalar bonds only.

The system equations for the WBGO are,

$$\Delta\dot{s}_1 = r_{1A}\dot{\theta}_A + r_{1P}\dot{\theta}_P; \quad \Delta\dot{s}_2 = -r_{2A}\dot{\theta}_A - r_{2P}\dot{\theta}_P \tag{21}$$

$$F_1 = K_{s_1}\Delta s_1 + R_{s_1}\Delta\dot{s}_1; \quad F_2 = K_{s_2}\Delta s_2 + R_{s_2}\Delta\dot{s}_2 \tag{22}$$

$$\tau_A = r_{1A}F_1 - r_{2A}F_2; \quad \tau_P = -r_{1P}F_1 + r_{2P}F_2 \tag{23}$$

The structure of the WBGO for a joint actuation string-tube module is as follows.

TABLE III

Output = WBGO for joint actuation string-tube (Input)

Parameters:	**C:**K_{s_1}, **C:**K_{s_2}, **R:**R_{s_1}, **R:**R_{s_2}, r_{1A}, r_{1P}, r_{2A}, r_{2P}
Initially required variables:	θ_A, θ_P
Input:	$\dot{\theta}_A$, $\dot{\theta}_P$
Output:	F_{s_1}, F_{s_2}, τ_A, τ_P based on (21)-(23).

C. WBGO for rotational coupling at prosthetic finger joints

The WBGO for the rotational coupling roughly outlined in Fig. 9 is elaborated in Fig. 12. The relative angular velocity ${}^{0}_{i-1}\overline{\omega}_i$ between links ***i*** and ***i-1***, and the torque ${}^{0}\overline{\tau}_i$ are transformed to ${}^{i-1}_{i-1}\overline{\omega}_i$ and ${}^{i-1}\overline{\tau}_i$ by the modulated multiport **MTF:** ${}^{0}_{i-1}R^T$. This changes the frame of expression from frame ***0*** to frame ***i-1***. Single bonds have been direct summed to obtain the multibond as shown. Input torque ${}^{i-1}\tau_{z_i\text{in}}$ at the *active joint* of the prosthesis is supplied by the *natural joint* to which it is connected. This results in motion of the *active joint*, which is transmitted to the string-tube subsystem, causing it to actuate the *passive* joint. The causal path clearly depicts this functioning. High values of stiffness ${}^{i-1}K_{\omega xi}$ and ${}^{i-1}K_{\omega yi}$ with matching values for ${}^{i-1}R_{\omega xi}$ and ${}^{i-1}R_{\omega yi}$ are used to prevent relative angular motion in these directions, instead of rigidly imposing constraints. A *passive joint* has a similar WBGO except for the absence of the bond supplying additional input torque.

D. Complete model of the hand prosthesis system using WBGO

Using the WBGO for the hand prosthesis system developed above, a complete model for the string-tube based two-joint prosthetic finger mechanism is assembled and depicted in Fig. 13. It is for general three-dimensional motion of the finger links, and not restricted to a planar case only. Four types of WBGO have been used in the complete model. Each WBGO has a bond graph structure which can be concealed to avoid excessive detail and confusion. Each WBGO interfaces with other appropriate WBGO using a combination of single and multibonds. It may be observed that an otherwise large model for the hand prosthesis system is now compactly represented. The clear picture of the overall system along with its component subsystems and their interactions has been preserved. The object oriented programming structure of each WBGO for the hand prosthesis system is conducive to simplified and rapid coding for numerical simulation.

IV. Conclusion

The hand prosthesis system is modeled using the bond graph approach. This system is too large to represent conveniently using either single or multibond graphs. To facilitate the modeling of this system using compact representation, the concept of WBG is applied to represent component subsystems as Objects. WBGO are compact representations of subsystems, within the overall dynamic system considered, with a well defined structure. The Object oriented programming structure of each WBGO facilitates coding for numerical simulation. The advantages of the WBGO have been discussed. WBGO are identified and analyzed for the hand prosthesis system. These include WBGO for the following subsystems: (1) rigid finger link dynamics, (2) translational coupling between two consecutive finger links, (3) rotational coupling between them, and (4) string-tube mechanics for *passive joint* actuation. The bond graph details for each WBGO have been presented together with a derivation of their systems equations and a tabulated outline of its structure.

ACKNOWLEDGMENT

This work has been supported by the Japan Society for the Promotion of Science (JSPS). The authors would like to express their gratitude to the referees for their detailed and useful comments.

REFERENCES

[Karnopp et al., 2000] D. C. Karnopp, D. L. Margolis, and R. C. Rosenberg, System Dynamics: Modeling and Simulation of Mechatronic Systems, 3rd ed., Wiley-Interscience, 2000.

[Mukherjee et al., 2000] A. Mukherjee, R. Karmakar, Modeling and Simulation of Engineering Systems Through Bondgraphs, Narosa Publishing House, New Delhi, 2000.

[Vaz and Hirai, 2003] A. Vaz and S. Hirai, "Actuation of a Thumb Prosthesis using Remaining Natural Fingers," Proceedings of the IEEE/RSJ Int. Conf. on Intelligent Robots and Systems (IROS 2003), Las Vegas, pp. 1998-2003, October 2003.

[Bonderson, 1975] L. S. Bonderson, "Vector Bond Graphs Applied to One-Dimensional Distributed Systems," *Journal of Dynamic Systems, Measurement, and Control*, Vol. 97, No. 1, pp. 75-82, 1975.

[Bonderson, 1977] L. S. Bonderson, "System Properties of One-Dimensional Distributed Systems," *Journal of Dynamic Systems, Measurement, and Control*, Vol. 99, No. 2, pp. 85-90, 1977.

[Breedveld, 1982] P. C. Breedveld, "Proposition for an Unambiguous Vector Bond Graph Notation," *Journal of Dynamic Systems, Measurement, and Control*, Vol. 104, No. 3, pp. 267-270, 1982.

[Breedveld, 1985] P. C. Breedveld, "Multibond Graph Elements in Physical Systems Theory," *Journal of The Franklin Institute*, vol. 319, No. 1/2, pp. 1-36, 1985.

[Tiernego and Bos, 1985] M. J. L. Tiernego and A. M. Bos, "Modelling the Dynamics and Kinematics of Mechanical Systems with Multibond Graphs," *Journal of The Franklin Institute*, vol. 319, No. 1/2, pp. 37-50, 1985.

[Bos and Tiernego, 1985] A. M. Bos and M. J. L. Tiernego, "Formula Manipulation in the Bond Graph Modelling and Simulation of Large Mechanical Systems," *Journal of The Franklin Institute*, vol. 319, No. 1/2, pp. 51-65, 1985.

[Jang and Han, 1998] J. Jang and C. Han, "Proposition of a Modeling Method for Constrained Mechanical Systems Based on the Vector Bond Graph," *Journal of The Franklin Institute*, vol. 335B, No. 3, pp. 451-469, 1998.

[Chao et al., 1989] E. Y. S. Chao, K. An, W. P. Cooney III, R. L. Linscheid, Biomechanics of the Hand, World Scientific: Singapore, 1989.

[Craig, 1989] J. J. Craig, Introduction to Robotics: Mechanics and Control, 2nd ed., Addison Wesley, 1989.

[Shames, 1996] I. H. Shames, Engineering Mechanics, Prentice Hall, 1996.

[Favre and Scavarda, 1998] W. Favre and S. Scavarda, "Bond Graph Representation of Multibody Systems with Kinematic Loops," *Journal of The Franklin Institute*, vol. 335B, No. 4, pp. 643-660, 1998.

[Karnopp, 1997] D. Karnopp, "Understanding Multibody Dynamics Using Bond Graph representations," *Journal of The Franklin Institute*, vol. 334B, No. 4, pp. 641-642, 1997.

[Zeid and Overholt, 1995] A. A. Zeid, J. L. Overholt, "Singularly Perturbed Formulation: Explicit Modeling of Multibody Systems," *Journal of The Franklin Institute*, vol. 332B, No. 1, pp. 21-45, 1995.

[Vaz and Hirai, 2004] A. Vaz and S. Hirai, "Application of Vector Bond Graphs to the Modelling of a Class of Hand Prosthesis," Proceedings of the 7th Biennial ASME Conference on Engineering Systems Design and Analysis (ESDA 2004), accepted for publication, Manchester, July 2004.

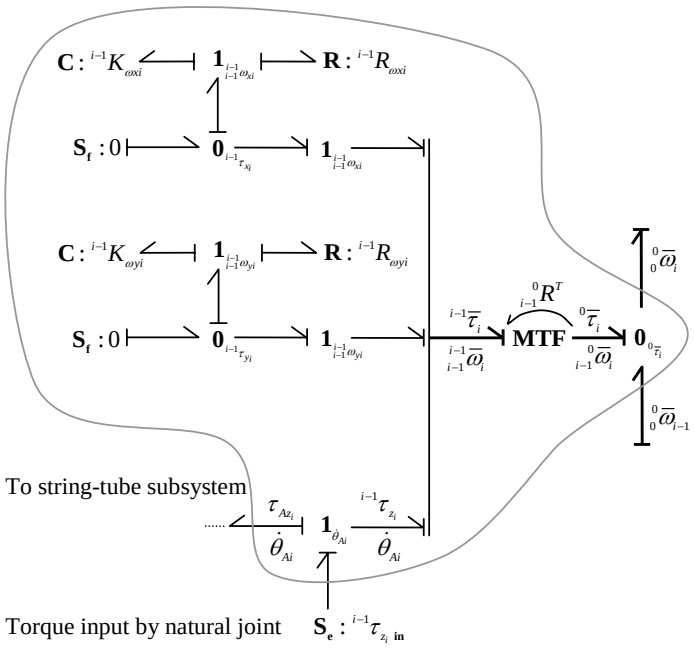

Fig. 12. WBGO for an active joint system.

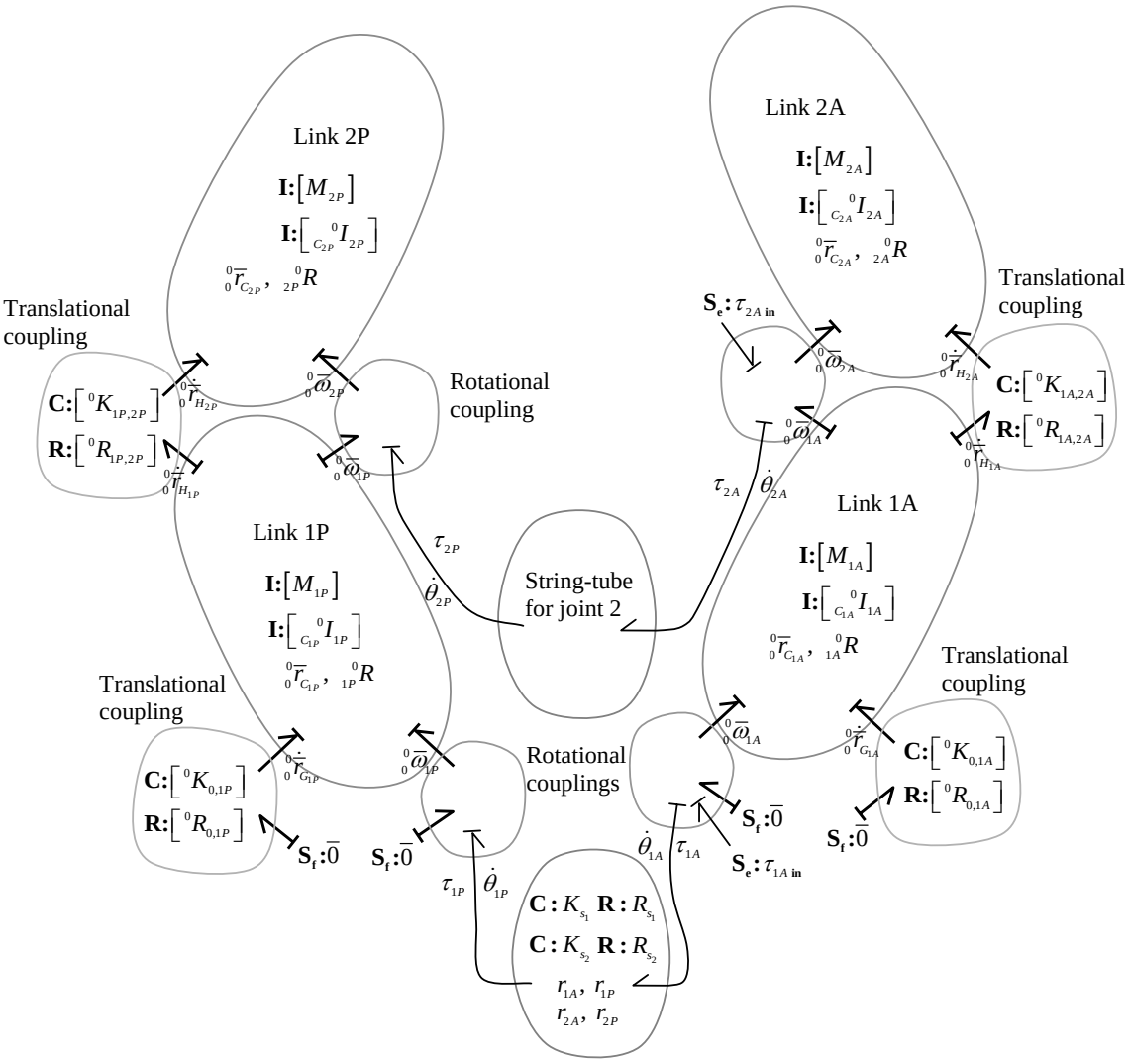

Fig. 13. WBGO used in modeling a string-tube based two-joint actuated finger prosthesis.